

Tetracycline-loaded Electrospun Poly(L-lactide-co- ϵ -caprolactone) Membranes for One-step Periodontal Treatment

*Thannaphat Jenvoraphot^{a,b}, Boontharika Thapsukhon^c, Donraporn Daranarong^d, Robert Molloy^e, Chayarop Supanchart^f, Suttichai Krisanaprakornkit^g, Paul D. Topham^h, Brian Tighe^h, Anisa Mahomed^h and Winita Punyodom^{*a,b,e}*

^a Department of Chemistry, Faculty of Science, Chiang Mai University, Chiang Mai, 50200, Thailand

^b Department of Chemistry and Center for Innovation in Chemistry, Faculty of Science, Chiang Mai University, Chiang Mai, 50200, Thailand

^c Division of Chemistry, School of Science, University of Phayao, Phayao, 56000, Thailand

^d Science and Technology Research Institute, Chiang Mai University, Chiang Mai, 50200, Thailand

^e Materials Science Research Center, Faculty of Science, Chiang Mai University, Chiang Mai, 50200, Thailand

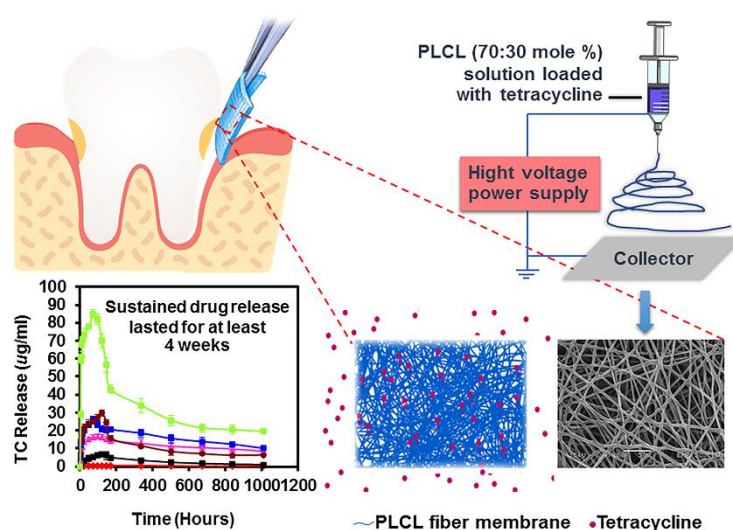
^f Department of Oral and Maxillofacial Surgery, Faculty of Dentistry, Chiang Mai University, Chiang Mai, 50200, Thailand

^g Department of Oral Biology and Oral Diagnostic Sciences, Faculty of Dentistry, Chiang Mai University, Chiang Mai, 50200, Thailand

^h Aston Institute of Materials Research, Aston University, Aston Triangle, Birmingham, B4 7ET, United Kingdom

* Corresponding Author's E-mail: winita.punyodom@cmu.ac.th

ABSTRACT



In this research, a one-step periodontal membrane, with the required function and properties has been designed as an alternative method of tissue regenerative treatments. Designed nanoporous prototypes from poly(L-lactide-*co*- ϵ -caprolactone) (PLCL, 70:30 mol%) were fabricated by electrospinning, denoted as S-PLCL. They were subsequently loaded with tetracycline (TC) in order to enhance periodontal regeneration and deliver an anti-inflammatory and antibiotic drug. It was found that TC loading did not have any significant effect on the fiber diameter but did increase hydrophilicity. With increasing TC loading, the water vapor permeability (WVP) of the S-PLCL membrane decreased within the range of 31 - 56% when compared with neat S-PLCL membranes, while in the solvent-cast film (F-PLCL) no significant change in WVP was observed. Moreover, S-PLCL demonstrated a controllable slow release rate of TC. S-PLCL loaded with 1,500 $\mu\text{g/ml}$ of TC showed a release concentration of 30 ppm over a certain time period to promote greater levels of human oral fibroblast (HOF) and human oral keratinocyte (HOK) cell proliferation and plaque inhibition. In conclusion, a TC-loaded S-PLCL fibrous membrane has been designed and fabricated to provide the ideal conditions for cell proliferation and antibiotic activity during treatment, outperforming non-fibrous F-PLCL loaded with TC at the same concentration.

Keywords: poly(L-lactide-*co*- ϵ -caprolactone), biodegradable, tetracycline, electrospinning, controlled release, periodontitis treatment, antimicrobial activity

1. INTRODUCTION

Periodontitis is an inflammatory disorder of the tissues surrounding the teeth. Inflammation in the periodontal tissue is initiated by the presence of microbial plaque and bacterial infections in the mouth such as *Actinobacillus actinomycetemcomitans*, *Porphyromonas gingivalis*, *Prevotella intermedia*, *Aggregatibacter actinomycetemcomitans*, *Treponema denticola* and *Tannerella forsythia*, etc.¹⁻⁵. An increase in optimal conditions encourages the formation of plaque, through bacterial release of acids and toxins from the body, an inflammatory reaction is stimulated in the oral periodontal tissue. This results in gingival inflammation, along with swelling and bleeding are a part of periodontal disease, which is known to cause periodontal tissue deterioration. Ultimately, this can lead to alveolar bone resorption as the teeth separate from the gingival tissue, which is referred to as the formation of periodontal pockets^{1,6-7}.

The utilisation of biopolymers has considerably impacted the preference of modern medicine^{2,8}. Specifically, biodegradable polymers provide a greatly advantage of broken-down and removable abilities after they have served their intended purpose. Applications for degradable polymers are wide-ranging, in particular they are used as surgical sutures and implants materials in clinic⁸. To meet the present optimal functional demand, materials with proper physical, chemical, biological, biomechanical and degradative properties must be selected⁸. However, periodontal surgery is often not undertaken by patients due to the fact that they continue to express concerns about the pain they will experience following surgical procedure. At present, the rate of patients refusing surgical treatment is increasing, with many patients expressing an interest in the use of drug therapies to avoid periodontal surgery^{2,9-11}.

Pharmacotherapeutics play an adjunctive role in the management of periodontitis patients. Adjunctive therapies are categorized by their route of administration to the diseased sites and may involve the use of systemic antibiotics¹². During the past two decades, dentists and microbiologists have attempted the use of periodontal antibiotic therapy to address specific bacterial infections in patients with periodontitis. The American Academy of Periodontology has offered guidelines for systemic and topical antibiotic use in treating periodontal disease¹³. These guidelines suggest that aggressive types of periodontitis and acute periodontal infections should be treated with systemic antibiotics, while chronic infections should be treated with topical therapy. In cases of aggressive periodontitis, systemic antibiotics may be used as an adjunctive form of therapy. Several lines of common antibiotics have been used in periodontal treatment

including tetracycline, ciprofloxacin, metronidazole and penicillin ^[14]. In particular, tetracycline has demonstrated a high degree of bacteriostatic activity against the specific anaerobic bacteria thought to cause periodontal disease ¹⁵⁻¹⁷. Tetracycline or tetracycline hydrochloride (TC) is a broad-spectrum antibiotic which contains a dimethylamine group at the C4 position in the ring A. Its existence is necessary to show antibiotic properties (see figure S1 in supporting information). TC is a protein synthesis inhibitor that binds to the bacterial 30S ribosome subunit and blocks the bond between tRNA and mRNA. It has been frequently used against gram-positive and gram-negative microorganisms, and is extensively used in antibiotics for human and veterinary use ¹⁸⁻²⁰.

At present, applications of biodegradable materials have increased due to the important properties they possess, such as a preferred degradation time and non-toxic degradation products. Resorbable guided tissue regeneration (GTR) and guided bone regeneration (GBR) membranes are currently on the market and have been widely considered for orthopaedic applications in both clinical and theoretical experiments¹. However, the use of these membranes may be subject to certain drawbacks such as inflammatory foreign-body reactions that are associated with their degradation and the absence of antibacterial activity ¹⁸.

To avoid surgical treatment and to increase the effectiveness of GTR and GBR membranes, a combination of a drug therapy and a resorbable membrane has been proposed as an alternative and convenient method of periodontal treatment. A suitable controlled release of a drug, such as tetracycline, may contribute to the faster regeneration of beneficial cells like osteoblasts, fibroblasts and other types of cells ^{18, 21}. Moreover, electrospinning is a simple method of fibrous polymer production with fiber diameters that are within a range of ca. 50 nanometers to several tens of μm ²¹⁻³⁰. Many biodegradable materials have been fabricated for use in medical applications via electrospinning and have been designed for the controlled release of drugs ¹⁸. TC has been loaded into poly(lactic acid), poly(caprolactone), cellulose and blends of each of the above during the electrospinning process to produce drug-loaded biomedical scaffolds. The prepared nanofibrous mats presented a sustained and suitable drug release rate, along with adequate levels of water uptake, permeability, antibacterial activities and good biocompatibility ^{18, 31}.

The objective of this research is to design a one-step periodontal membrane that can guide regeneration of bone and tissue, while exhibiting anti-inflammatory and antibacterial properties. To this end, nanoporous membrane prototypes have been

designed and fabricated by electrospinning. They were then modified by drug loading to enhance periodontal regeneration when compared to the film casting technique. These designed prototypes are expected to promote antibiotic properties and facilitate the controlled release of drugs over a suitable period of time during the course of treatment.

2. EXPERIMENTAL PROCEDURE

2.1 Materials and Methods

2.1.1. Materials

L-lactide was purchased from Bioplastics Production Laboratory for Medical Applications, Faculty of Science, Chiang Mai University, Thailand, while ϵ -caprolactone was purchased from Sigma-Aldrich (St Louis, MO, USA). Chloroform, methanol and ethyl acetate were acquired from RCI Labscan (Bangkok, Thailand). Tetracycline hydrochloride (TC) was obtained from Bio Basic Inc (Markham, Canada). The alamarBlue reagent was acquired from Bio-Rad Laboratories (California, US).

2.1.2. Polymer Synthesis and Characterization

Poly(L-lactide-*co*- ϵ -caprolactone), PLCL with 70:30 mole % (medical grade) was synthesized by following the previous studies (see structure (figure S1) in supporting information)³²⁻³⁵. The copolymer was obtained as white solid granules with >80% yield. To confirm that the obtained PLCL copolymer met the requirements of a medical-grade polymer, the copolymer was characterized according to the requirements of ASTM F1925-17³⁶.

2.1.3. Preparation of PLCL-loaded TC Drug Membranes

For the preparation of electrospun membranes (S-PLCL) loaded with tetracycline (TC), a clear and homogenous 20 mL of 16% w/v PLCL solution was performed following the previous studies³²⁻³³. Subsequently, TC was added into PLCL solution at various concentrations of 0, 250, 500, 750, 1500 and 2500 μ g/ml to the polymer solution and stirred at room temperature overnight. PLCL membranes with various TC loadings were then fabricated by electrospinning at a fixed voltage of 15 kV and a needle-to-collector spinning distance of 15 cm. Aluminum foil was used as a ground collector. The electrospun membranes were collected after 20 mL of each polymer solution had been ejected. Under the processing conditions employed, the average thickness of the nanofiber samples obtained was about 0.30 mm.

For the solution-cast film membranes (F-PLCL) loaded with various tetracycline (TC) concentrations, the PLCL copolymer at a concentration of 0.5% (w/v) was dissolved in 20 mL of chloroform and then various amounts of TC added (0, 250, 500, 750, 1500 and 2500 $\mu\text{g/ml}$). The solutions were stirred overnight at room temperature for complete dissolution. Each solution was then poured into a glass petri dish and the solvent allowed to evaporate slowly in air at room temperature for 48 h. The average thickness of the film samples obtained was approximately 0.20 mm.

Finally, both the S-PLCL and F-PLCL membranes with various degrees of TC loading were dried under vacuum at room temperature, removed and allowed to stand to equilibrate to constant weight (*ca.* 24 h). The surface morphology of the membranes, together with their fiber diameters, were examined using scanning electron microscopy (SEM, JEOL 5910 LV)³²⁻³³.

2.1.4. Membrane Characterization

Water Contact Angle

The hydrophilicity of the membrane was measured through water contact angle using a homemade apparatus and analysed by the Protractor software. S-PLCL and F-PLCL membranes were cut into 50 \times 50 mm segments and attached to glass slides. Water droplets were placed on the membrane and their contact angles with the membranes were measured ($n = 5$).

Water Vapour Permeability (WVP)

WVP was measured using a modified version of the ASTM method (ASTM E96-E80) as described by Shiku *et al.*³⁷. The samples were incubated in an oven at 37.0 \pm 1.0 $^{\circ}\text{C}$ and at a relative humidity (RH) of 50 \pm 5% for 48 hours before the experiment. Circular-shaped test specimens were cut from the S-PLCL and F-PLCL membranes with 40 \times 40 mm². The S-PLCL and F-PLCL membranes were sealed to a permeation aluminium cup containing silica gel (0% RH) with silicone vacuum grease and a rubber gasket to hold the membranes in place. The cups were placed in a desiccator containing distilled water at 37.0 \pm 1.0 $^{\circ}\text{C}$ with 50 \pm 5 %RH, which effectively mimicked the average temperature of the body. Cups were then weighed every 24 hours for 7 days with regular weighing until a steady state was reached. WVP values of the S-PLCL and F-PLCL membranes were calculated as follows:

$$\text{WVP (gm}^{-1}\text{s}^{-1}\text{Pa}^{-1}) = w_1A^{-1}t^{-1}(P_2-P_1)^{-1}$$

where w represents the weight gain of the cup (g); l represents the membrane thickness (m); A is the exposed area of the membrane (m^2); t is the time of gain (s); P_2 and P_1 are the corrected partial pressure at the inner surface of the membrane and the pressure of the surface of desiccant (Pa).

In Vitro Drug Release Study

The tetracycline drug (TC drug) release rate was analyzed using an Ultraviolet-Visible spectrometer (UV-Vis) as the method provided in previous studies^{22, 38}. The tested membranes, S-PLCL and F-PLCL with various TC loadings, were cut into 15×15 mm^2 pieces and accurately weighed. The release behavior of TC from the loaded membranes was studied in PBS buffer. All samples were analysed in triplicate. Samples without drug were used as controls. The prepared samples were fully immersed in a vial containing 5.00 mL of PBS at 37 °C. At specific time intervals (0-1008 hrs), aliquot samples were collected from the incubation buffer and 3.00 mL used to measure their absorbance at 364 nm (λ_{max}) by UV spectroscopy (UV 3600 Shimadzu Spectrophotometer). Concentrations of released TC were obtained at different times and were calculated using the standard curve of the concentration *versus* absorbance with an r^2 value of 0.9999 (data not shown) and the cumulative concentrations were calculated accordingly.

In Vitro Hydrolytic Degradation Studies

Various TC-loaded S-PLCL and F-PLCL membranes were cut into 15×15 mm^2 pieces and accurately pre-weighed before study. The samples were incubated in PBS at a temperature of 37.0 °C for 6 weeks. At designated time intervals throughout the 6-week period, the pH of the PBS was also measured. Reductions in both S-PLCL and F-PLCL sample weights were determined as a function of time ($n = 3$).

Biological Evaluation Studies

The effects of polymer topology and TC drug loading of F-PLCL and S-PLCL membranes on human oral fibroblast (HOF) and human oral keratinocyte (HOK) cell response were studied to evaluate the potential of these membranes in biomedical applications and for periodontitis treatment. The HOF and HOK cells were cultivated and cell populations of approximately 1×10^5 cells ml^{-1} (70% confluence) were used to seed S-PLCL and F-PLCL membranes^[39]. At periodic intervals times, samples were rinsed

with PBS solution and trypsin (2.5 %v/v) solution were then added. The samples were incubated for cells removing at $37.0\pm 0.1^{\circ}\text{C}$ for 7 mins. Cell viability was subsequently calculated using the 0.2% Trypan Blue and a hemocytometer. All samples were evaluated in triplicate ($n = 3$).

Metabolic Activity of Cell

A fixed number (1×10^5 cells ml^{-1}) of HOF and HOK cells were plated into 96-well plates containing S-PLCL and F-PLCL membranes and incubated for 24 hours ($37.0\pm 0.1^{\circ}\text{C}$, 5% CO_2). Metabolic activities in the HOF populations were evaluated by 20 μl of alamarBlue solution added to each well, and they were then further incubated for an additional 3 hours ($37.0\pm 0.1^{\circ}\text{C}$, 5% CO_2). The alamarBlue analyses were performed at 540/600 nm wavelengths^[40]. Mean values of 5 samples were determined ($n = 5$).

Lactate Dehydrogenase (LDH) Assay

The integrity of S-PLCL and F-PLCL membranes was assessed through the leakage of LDH, where 10 μl of lysis solution was added the well-plates for 45 minutes before the endpoint, to serve as a positive control. The well-plates were subsequently centrifuged and a 50 μl sample of the supernatant was then transferred to a sterile 96 well-plate with 100 μl of LDH mixture before they were incubated in the dark for 30 minutes. Absorbance at 490/690 nm was recorded using a microplate spectrophotometer and the mean value of 5 samples was then determined ($n = 5$)^{32, 35, 41}.

In Vitro Antimicrobial Activity Evaluation

Three dental samples of plaque were provided by the Faculty of Dentistry, Chiang Mai University. The plaque samples were grown anaerobically at $37\pm 0.1^{\circ}\text{C}$ in Brain Heart Infusion (BHI) broth for 24 hours. After incubation, the growth of the bacteria in the dental plaque samples was confirmed by observing the colony characteristics under a microscope. The concentration of the bacteria was adjusted with BHI broth before this was used in the experiments, following the standard guidelines⁴²⁻⁴³. Aqueous solutions containing S-PLCL with various degrees of TC loading were separately prepared in deionized water and diluted in BHI broth containing the test plaque. Aqueous solutions containing F-PLCL with various degrees of TC loading were also prepared in a similar manner. The polymer samples were examined after 24 hours of incubation at $37\pm 0.1^{\circ}\text{C}$

and the colony-forming units (CFUs) were evaluated. Experiments for all samples were conducted in triplicate.

Statistical Analysis.

All statistical evaluations were performed using two-way ANOVA analysis and Bonferroni post hoc test (significance level < 0.05).

3. RESULTS AND DISCUSSION

3.1. Polymer Characterization

A PLCL copolymer in the ratio of LL:CL = 70:30 mol% has been synthesized and $> 80\%$ yield was obtained. This ratio was chosen from a previous study as it leads to the optimum material properties among a range of PLCL with ratios ranging from 50:50 to 70:30 mol%³⁴. The membranes should be able to maintain their shape (i.e., dimensionally stable fibers) for at least 1–3 months during treatment and be stable during storage for potentially long periods at room temperature before use. Therefore, PLCL 70:30 mol%, with its higher glass transition temperature and partial crystallinity to stiffen the copolymer matrix, was chosen for this study.

To confirm the suitability of the PLCL copolymer for medical applications, the properties of the PLCL copolymer were characterized using ASTM F1925-17. The results are presented in Table 1. Briefly, the copolymer composition determined by 400 MHz ¹H-NMR spectroscopy (Bruker DPX-400 NMR spectrometer, Switzerland) demonstrated that LL:CL = 72.5:27.5 mol%. This was consistent with the requirement that the molar ratio should fall within a range of ± 3 mol% from the initial co-monomer feed ratio of LL:CL (70:30). The intrinsic viscosity, $[\eta]$, as determined by dilute-solution viscometry (0.5 %w/v, 30°C, in chloroform (CHCl₃)), was recorded at 1.86 dl/g. Thermal transitions and degree of crystallinity were determined by differential scanning calorimetry (DSC) (Perkin-Elmer DSC7). The appearance of a melting transition in the DSC thermogram with a T_m (peak) of 147.8 °C and a crystallinity value of 27.3 %.

Table 1. Physical and chemical property measurements, compared with the ASTM F1925-17 specification, for the medical-grade PLCL copolymer.

Specification	ASTM F1925-17	PLCL
Residual Monomer	< 2.0 %	0.15% Total (0.15% LL,0.00%CL)
Residual Solvent	< 1000 ppm	> 1 ppm
Heavy Metals	≤ 10 ppm	1 ppm
Residual Catalyst (Optional)	≤ 150 ppm	60 ppm
Residual Water (Optional)	≤ 0.5 %	0.02 %
Copolymer Ratio (molar ratio)	± 3 % of target	2.38 % (72.5:27.5)

From the results shown in Table 1, the total residual monomer, solvent, catalyst and water content were all within the stated limits. Residual L-lactide (LL) and ϵ -caprolactone (CL) monomers (%) and solvents (ppm), as determined by gas chromatography with a flame ionization detector (GC-FID) using methylene chloride as solvent and 2,6-dimethyl- α -pyrone as an internal standard, were well below the maximum quantities permitted of 0.15% of total residual monomers and less than 1 ppm of total residual solvents for ethyl acetate and toluene (see supporting information). Residual heavy metal (Pb) and catalyst (Sn) contents were measured using inductively coupled plasma-optical emission spectroscopy (ICP-OES) by Intertek testing services (Thailand) Ltd. and were found to be 1 and 60 ppm respectively. To confirm the moisture content in the PLCL copolymer, Karl Fischer Titration at 150°C was used to determine that the residual water content of PLCL was 0.02 %.

According to the results, the characterization of PLCL met the ASTM F1925-17 property requirements for a medical grade copolymer to be used in medical devices. Therefore, it was further used for fabrication of a periodontal membrane.

3.2. Preparation of PLCL-loaded TC Drug Membranes

In this study, electrospinning and solvent casting techniques were used to produce porous S-PLCL and non-porous F-PLCL membranes, respectively. The S-PLCL

membranes were white and opaque with a thickness of 0.30 ± 0.03 mm, while F-PLCL membranes were transparent with a thickness of 0.20 ± 0.03 mm. For S-PLCL, a porous surface with random nanofibers was observed by SEM (figure S3 in supporting information). Similar to a previous report, electrospinning was used to mimic the architecture of the extracellular matrix (ECM), where the randomly aligned nanofibers promoted cell growth, proliferation and differentiation³⁵. In the present study, PLCL copolymer solutions at a concentration of 16% (w/v) were used to produce S-PLCL membranes which were bead-free, well-defined nanofibrous membranes.

In this study, we evaluated the effect of TC drug loading on the diameter of the electrospun fibers within the S-PLCL membranes. The TC drug loading appears to have a very small effect on the electrospun fiber morphology (Figure 1a). Loading the S-PLCL membranes with 250, 500, 750, 1,500 and 2,500 $\mu\text{g/ml}$ resulted in mean fiber diameter values of 619.0 ± 10.4 , 604.3 ± 28.4 , 603.4 ± 14.1 , 569.6 ± 13.1 , and 562.2 ± 31.6 nm, respectively, while the S-PLCL membrane without TC drug was 624.3 ± 28.4 nm (Figure 1b). At lower drug loadings (250, 500 and 750 ppm), the concentration of TC did not significantly affect the diameter of the fibers as the differences were within experimental error (0.9, 3.2 and 3.3 %, respectively), when compared to the S-PLCL membrane without TC loading, while higher TC loadings of 1,500 and 2,500 $\mu\text{g/ml}$ decreased the mean diameter by 8.8 and 9.9 %, respectively. This relatively small effect illustrates that the fiber morphology is predominantly determined by the electrospinning parameters for the polymer (*i.e.* concentration, solvent, voltage, ejection speed, needle-to-collector distance, type of collector and humidity), which allows one to incorporate substantial quantities of drug whilst having full control over the fibrous structure.

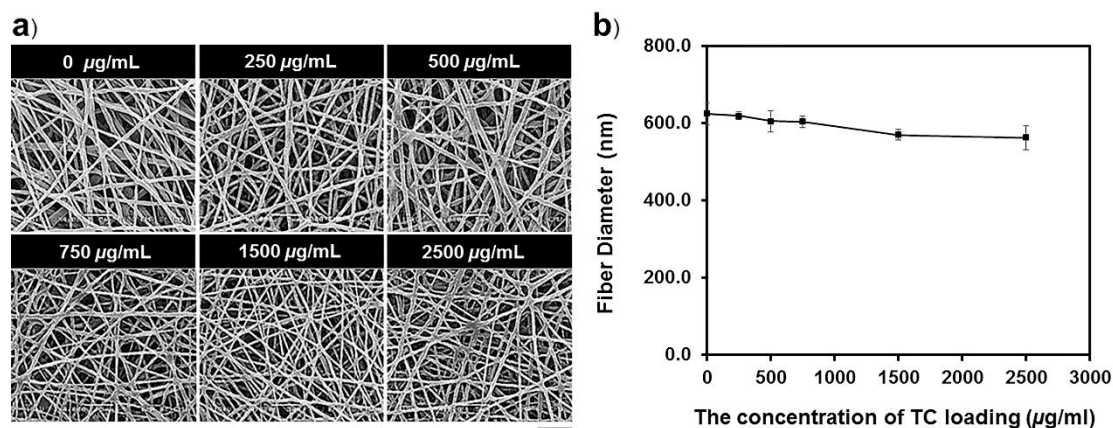


Figure 1. (a) SEM images of electrospun nanofibrous meshes of S-PLCL and S-PLCL with various TC drug loadings (Magnification $\times 4000$, thick black bar equal $5\ \mu\text{m}$) and (b) changes in the average fiber diameter of S-PLCL membranes loaded with TC drug ($\mu\text{g/ml}$).

3.3 Membrane Characterization

3.3.1 Water Contact Angle

The influence of cellular adhesion and proliferation depends upon the hydrophilicity of biomaterials as well as the surface morphology of their devices^{35, 45}. The release of drug from biodegradable polymers is known to be governed by the relative rates of erosion and diffusion mechanisms. Most biodegradable polymers used for drug delivery are degraded by hydrolysis. As the functional of hydroxyl groups break the ester bonds in the polymer chain, the physical integrity of the polymer degrades and allows the drug to be released³⁸. The TC loaded S-PLCL and F-PLCL membranes showed interesting wettability characteristics due to the TC drug being hydrophilic while the PLCL is predominantly hydrophobic. As the TC loading for both the S-PLCL and F-PLCL increased, the water contact angle decreased indicating that the presence of the drug increased the hydrophilicity of the membrane as expected (Figure 2). S-PLCL electrospun membranes with 1,500 and 2,500 $\mu\text{g/ml}$ TC loading exhibited water contact angles of $90.0\pm 0.0^\circ$ and $70.9\pm 0.1^\circ$, respectively, while the PLCL electrospun membranes were more hydrophobic with a mean water contact angle of $114.5\pm 0.3^\circ$. Meanwhile, F-

PLCL with 1,500 and 2,500 $\mu\text{g/ml}$ TC loading showed water contact angles of $70.8\pm 0.1^\circ$ and $65.6\pm 0.2^\circ$, respectively.

In comparison with F-PLCL, TC-loaded S-PLCL electrospun membranes were significantly more hydrophobic, except for the highest TC loading (2,500 $\mu\text{g/ml}$), where the water contact angles were more comparable. Pristine F-PLCL displayed a water contact angle of $86.2\pm 0.3^\circ$, which was lower than non-loaded S-PLCL by 25%, and this trend continued when loaded with 250-1500 $\mu\text{g/ml}$ of the TC drug. These results can be explained by entrapped air in the surface pores within the nanofibrous structure of TC-loaded S-PLCL, resulting from the electrospinning process, which can even be used to generate superhydrophobicity^{33,46,47}. It is also important to note that these values may have also been influenced by the presence of pores under the water droplets in the various fibrous morphologies, as reported elsewhere^{35,48}. This superhydrophobicity property can be beneficial in preventing bacterial adhesion, but is not always sustainable. It can be diminished, or even lost, when the surface is physically damaged⁴⁷. Therefore, it is clear that loading TC in PLCL can influence the morphology and hydrophobicity of the membranes and that this is likely to have consequences for the drug release profile, cell attachment and proliferation.

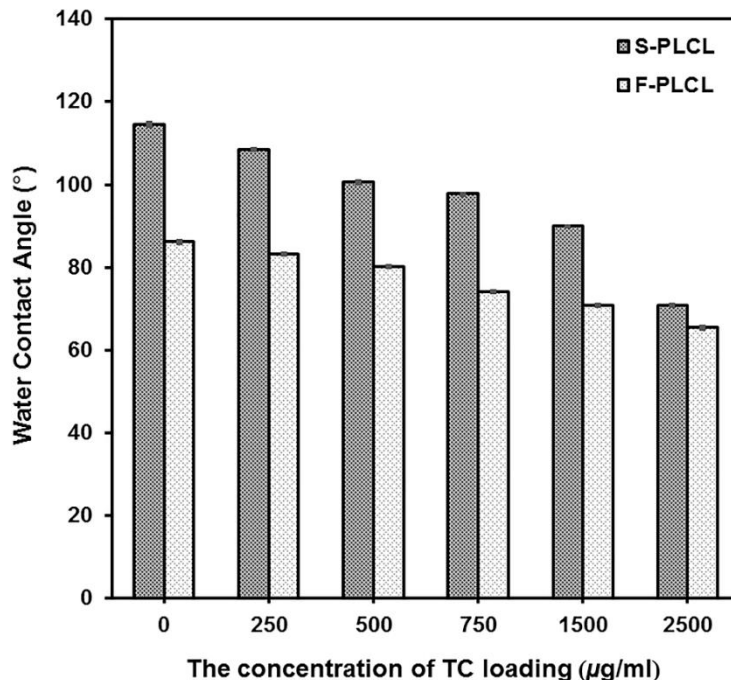


Figure 2. Effect of TC drug loading on the water contact angle of PLCL electrospun fabric (S-PLCL) and film (F-PLCL) membranes.

3.3.2 Water Vapor Permeability (WVP)

WVP is a measure of the amount of moisture that passes through a unit area of material per unit time. The barrier properties of the membranes are relevant to their applications by understanding the relationship between composition, structure, processing, and properties. The barrier performance of the S-PLCL and F-PLCL membranes with various TC drug loadings in terms of WVP is compared in Figure 3. In this study, WVP measurements were performed on the porous (S-PLCL) and non-porous (F-PLCL) membranes at various TC loadings. It was found that TC loading in the S-PLCL electrospun membranes tended to significantly decrease the WVP within a range of 31.35-56.02% when compared with the neat PLCL electrospun membranes ($48.41 \pm 10.21 \times 10^{-5} \text{ g mm/m}^2 \text{ s kPa}$) (Figure 3(a)). However, increasing the TC loading in the F-PLCL non-porous membranes did not significantly affect the WVP (Figure 3(b)). As expected, the WVP of S-PLCL (with and without the TC drug) were all higher than those of the F-PLCL membranes. Due to the differences in dispersion of the drug in S-PLCL and F-PLCL, the F-PLCL layer acted as a poor diffusion barrier resulting in the drug being trapped on the surface of the polymer rather than inside, thereby giving rise to a hydrophilic surface. In contrast, the S-PLCL membrane dispersed the drug around each layer of the S-PLCL membrane, which then facilitated good dispersion in the porous membranes⁴⁹. Moreover, incorporation of TC into the S-PLCL membranes reduced the WVP as the TC drug concentration increased from 250 to 2,500 $\mu\text{g/ml}$. This reduction in WVP could be attributed to the effect of the drug on the fiber within the internal structure of the membrane more than the effect on the diameter of the fibers. However, previous studies also reported that a reduction in the number of fibers and pores can reduce the water vapor diffusion through the membrane resulting in a decrease in water permeability⁴⁹⁻⁵¹.

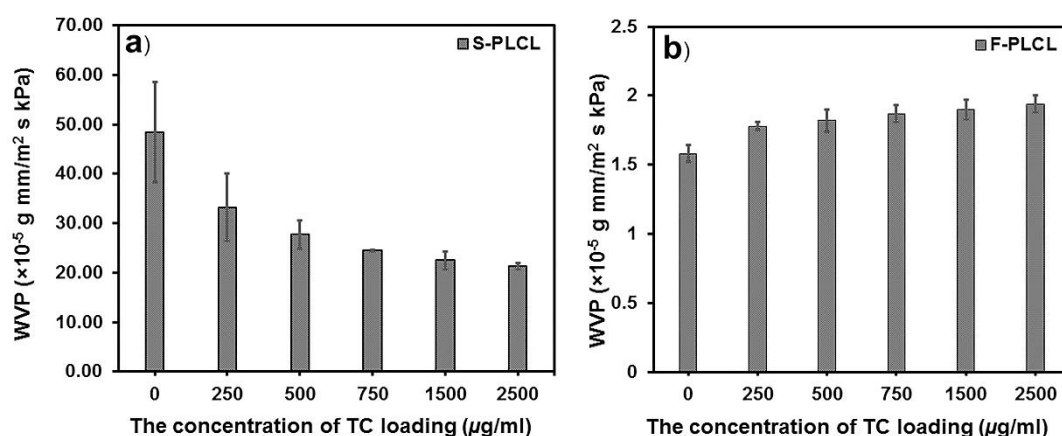


Figure 3. Water vapor permeability (WVP) of (a) S-PLCL and (b) F-PLCL membranes at TC loadings of 0, 250, 500, 750, 1,500 and 2,500 $\mu\text{g/ml}$

3.3.3. *In vitro* Drug Release behaviour

The profiles of the TC release rates for the S-PLCL and F-PLCL samples containing varying amounts of the TC drug (250, 500, 750, 1,500 and 2,500 $\mu\text{g/ml}$) were obtained in the presence of PBS at a pH of 7.4 for just over 1000 hours as shown in Figure 4. All of the samples exhibited a two-stage (bimodal) drug-release profile that was similar previous studies³¹. S-PLCL and F-PLCL with 2,500 $\mu\text{g/ml}$ TC loading exhibited the highest drug release rate, this correlated with the highest concentration value. The two membranes exhibited a burst release phase of 84.9 and 94.8 $\mu\text{g/ml}$, respectively, for TC released by 72 hours. The sustained release phase continued and terminated at 1,008 hours, by this time the remaining loaded drug was ultimately released. The release profiles of the S-PLCL membrane containing various amounts of the TC drug (250, 500, 750, 1,500 and 2,500 $\mu\text{g/ml}$) significantly affected the drug release rate as is shown in Figure 4(a). A greater amount of the drug content resulted in a faster drug release rate over the course of a 72 to 168 hour period. The drug release profile of a polymer matrix (as in S-PLCL and F-PLCL membrane) can be explained by the Fickian diffusion mechanism, which considers the drug penetration as the most important factor in drug release. Other mechanisms can be applied for the rate of drug release such as the release from the surface of the nanofibrous scaffold or the degradation of the polymer matrix⁵²⁻⁵³. It is believed that with increasing concentrations of TC, the dissolved drug in the polymer solution

exhibited a greater tendency to migrate to the surface or near the surface of nanofibers during the electrospinning process. Therefore, the exposure and diffusion of the TC from S-PLCL to the buffer solution tended to increase at 168 hours leading to a faster drug release rate. Moreover, the sustained drug release was lasted for a duration of 4 weeks. In general, the total percentage release from the cast films was lower than that of the electrospun membrane, as would be expected due to the much lower surface area of the former. Interestingly, when compared with F-PLCL, S-PLCL exhibited slower initial burst release values of between 60 to 144 hours. The cumulative TC release content of F-PLCL at 24 hours was $94.8 \pm 2.7 \mu\text{g/ml}$ from the initial loading with $2,500 \mu\text{g/ml}$, while S-PLCL was $73.7 \pm 1.8 \mu\text{g/ml}$. For F-PLCL the initial burst release of TC is attributed to the diffusion of the drug located near the surface, in addition F-PLCL membranes are more hydrophilic and associated with higher WVP values than S-PLCL. This slow-release rate of S-PLCL could be attributed to its partial crystallinity that resulted from its fabrication process, which limited the diffusion of the aqueous environment into the polymer layers and consequently limited the diffusion of the drug from the nanofibers.

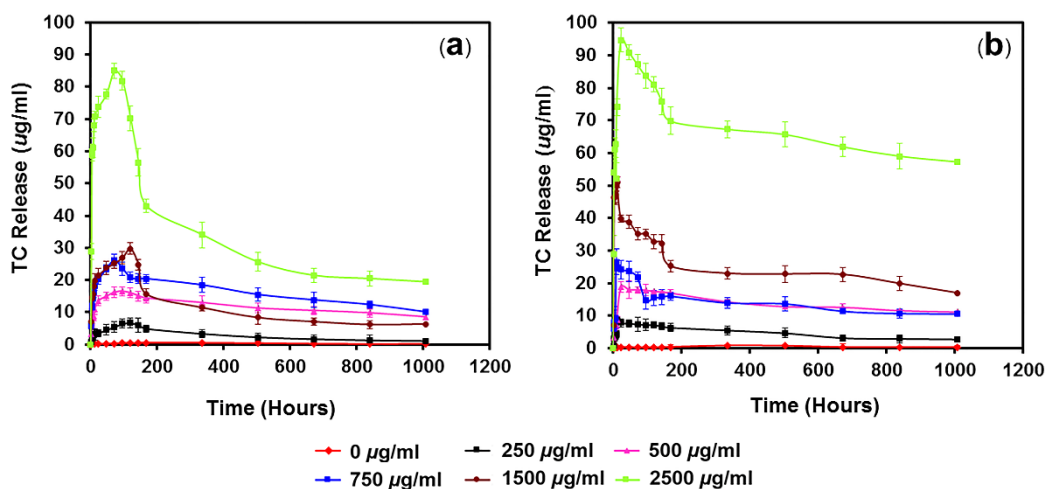


Figure 4. Time and TC drug release of (a) S-PLCL and (b) F-PLCL membranes at various degrees of TC loading

3.3.4 *In Vitro* Hydrolytic Degradation

The % weight retentions of S-PLCL and F-PLCL membranes at the end of a period of 6 weeks are shown in Figures 5 (a) and (b), respectively. It can be implied that

at the early stages of degradation, the S-PLCL membrane exhibited a surface erosion pattern due to the fact that it was fabricated from non-woven fibers with high surface area. Thus, the water molecules could penetrate more easily and degradation would then occur more easily. After this, the S-PLCL membrane surfaces were more hydrophilic, which resulted in faster water diffusion into the fiber matrix. The % weight retention values reached about 90-95 % after 6 weeks and 50% after 24 weeks of degradation. The F-PLCL membranes exhibited faster surface erosion patterns compared to S-PLCL membranes. This is because the diffusion of the drug to near the film surface made the F-PLCL membranes more hydrophilic. The % weight retention values of the F-PLCL membranes was about 80-90% after 6 weeks but decreased to 30% after 24 weeks of degradation.

The large degree of weight loss that occurred in the amorphous membrane region can be attributed to many random chain cleavages or pH changes. For S-PLCL, according to the semi-crystalline morphology, the amorphous phase was degraded first and then the crystalline phase was later degraded³⁴. Hence, the % weight retention slowly decreased which corresponded to a decrease in the pH value along with the time interval. The crystalline morphology in the semi-crystalline sample defined the pathways for chain cleavage, which induced a much slower process for weight loss. Thus, it has been proposed that the weight loss in the semi-crystalline sample primarily occurred in the amorphous gap regions between the crystal lamellar stacks⁵⁴.

The pH function of degradation time during *in vitro* hydrolytic degradation in PBS at $37.0 \pm 0.1^\circ\text{C}$ of the S-PLCL and F-PLCL membranes, are shown in Figures 5 (c) and (d), respectively. The pH decrease over time corresponds to mass loss that occurs due to the presence of acid-degraded products. While the hydrolytic degradation continues to take place, some amorphous regions in the S-PLCL undergo crystallisation and cause a decrease in the rate of that degradation. Due to the hydration taking place in the amorphous regions, at the end of week 24, the pH values of S-PLCL and F-PLCL exhibited dramatic decrease reaching 3.86 and 3.66 at a TC concentration of $500 \mu\text{g/ml}$, while other concentrations of TC decreased by about 40-50%. In accordance with the pH changes that occur during the first 6 weeks of degradation of the both of S-PLCL and F-PLCL membrane, the main factor that had a significant effect on the pH change was the fast mass loss that produced acidic side products from the degradation of esters in the polymer chain. It can be speculated that the reversal in the pattern for pH change for drug loadings of different concentration, as observed in the S-PLCL, is due to the presence of

hydroxyl groups in the molecular structure of TC which also affects the pH of PBS. Notably, the TC drug released from the S-PLCL membrane could maintain high drug concentrations over longer periods of time. The pH values of the PBS solution were dependent upon the degradation products obtained from the PLCL membrane. The S-PLCL membrane possessed a 3D fibrous network that allowed water molecules to penetrate through the membrane and accelerate degradation more efficiently than the F-PLCL membrane. Some TC drug molecules could be dissolved and emerge from the fiber into the PBS solution, which would then result in a decrease in pH values.

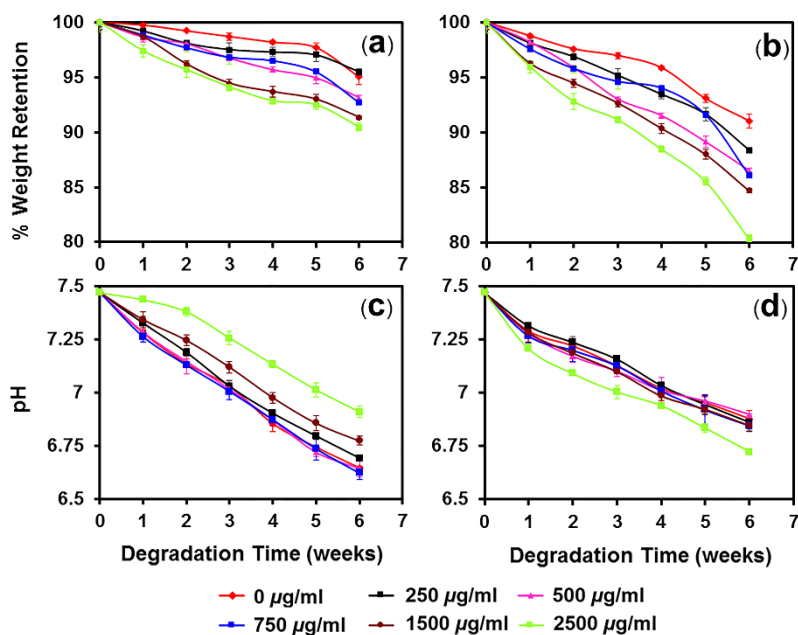


Figure 5. Weight retention values for the (a) S-PLCL and (b) F-PLCL membranes and pH decreases for (c) S-PLCL and (d) F-PLCL membranes in accordance with various TC drug loading concentration in $\mu\text{g/ml}$ during *in vitro* hydrolytic degradation

3.5. Biocompatibility Evaluation

3.5.1 Metabolic Activity of HOF and HOK Cells

For the intended medical application of the modified scaffold, it is essential to ensure that they are safe and non-toxic. Therefore, cytotoxicity tests were performed using human oral fibroblasts cells (HOF) and human oral keratinocyte (HOK) cells, which are key structural cells within the oral cavity. These are among the first cell types that would encounter the dental scaffold and are important in regulating the immune response and play an important role in oral wound healing⁵⁵. Thus, cell attachment and proliferation were assessed by performing the alamarBlue assay in order to evaluate the

potential toxicity of S-PLCL and F-PLCL, either with or without TC drug loading (Figure 6). According to ISO 10993-5, 2009, for a medical device to be considered non-cytotoxic, it must show a cell viability equal to or >70% of the negative control (mock extract, i.e., medium subjected to the same treatment as test extracts). With regard to the results shown in figure 6, it can be inferred that S- PLCL and F-PLCL with loaded TC values were non-cytotoxic to HOF cells, but were intrinsically cytotoxic for HOK cells. By increasing the concentration of the TC-loading in the membranes, cell viability was reduced with both the HOF and HOK cells. Previous reports have shown that proliferation of the integrin subunits in human fibroblasts were different from those of normal human keratinocytes⁵⁶⁻⁵⁸. However, it is unclear as to why the attachment and proliferation of HOF cells adhered to the S-PLCL and F-PLCL was superior to those of HOK cells. It is generally accepted that diverse cellular responses to synthetic surfaces can arise from differences in the adsorption of extracellular matrix (ECM) proteins to the surface. Different classes of cell adhesion receptors are known to mediate interactions between the cells and neighboring cells and the surrounding ECM. Among these receptors, integrins primarily mediate interactions between cells and ECM components, and transmit biochemical signals across the plasma membrane. It is well known that the integrins expressed on cell surfaces differ among cells or cell types, and that three major integrins, $\alpha_2\beta_1$, $\alpha_3\beta_1$, and $\alpha_6\beta_4$, are expressed in the normal basal keratinocyte layer^{56,59}.

Consistent with the difference in surface morphology, the electrospun membrane (S-PLCL) exhibited significantly higher viability of the attached cells than the film membrane (F-PLCL). This result can be explained by the difference surface topologies of the S-PLCL and F-PLCL membranes. The roughness of the S-PLCL membranes differed considerably, whereas the F-PLCL membrane exhibits a much smoother topographical profile. A smoother profile suggests that fewer sites for surface-cell interactions are available and consequently F-PLCL membrane results in a lower degree of cellular adhesion than the S-PLCL membrane. It can thus be concluded that the S-PLCL membrane with TC drug loading could be considered to be adequately biocompatible for dental scaffold purposes. Significantly, it was found to contain the best surface properties to enhance initial cell attachment in this study, given that an increased surface area enhances cellular adhesion.

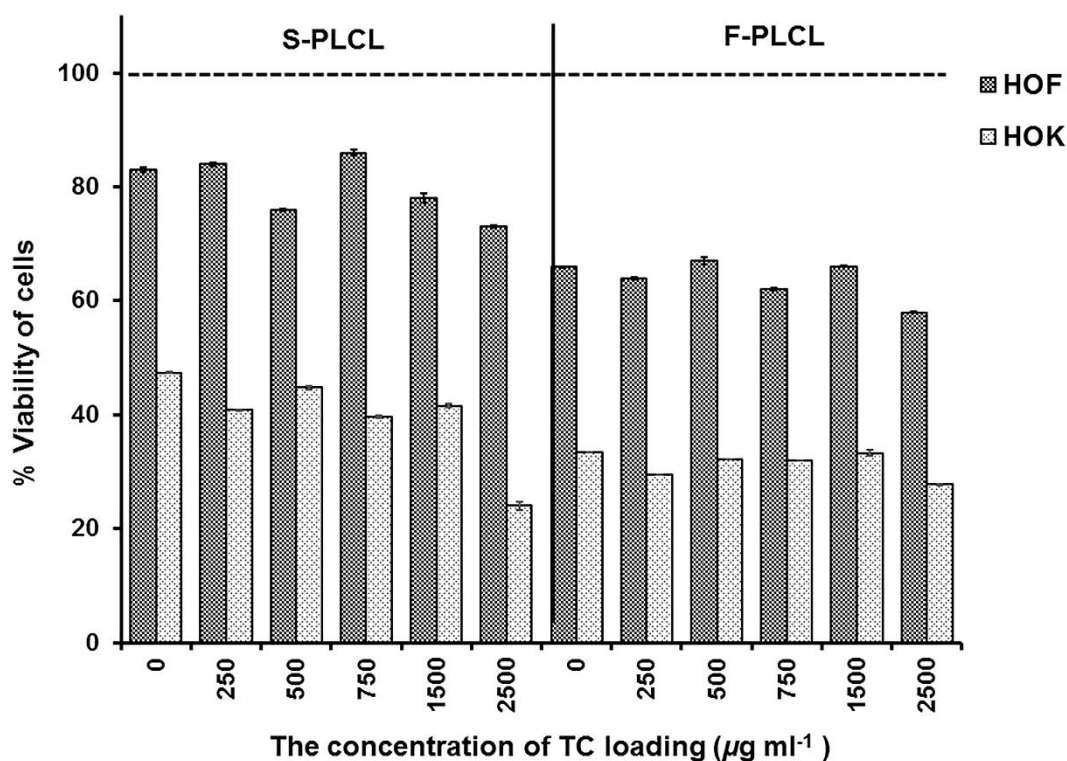


Figure 6. Indirect cell metabolic activity of (■) HOF and (□) HOK cells cultivated on S-PLCL and F-PLCL membranes at various TC-loading values for 24 hours measured by alamarBlue assay, with cells in asynchronous growth assigned at 100%.

3.5.2 Lactate Dehydrogenase (LDH) Assay

Membrane leakage of LDH into the medium provides an indication of cellular cytotoxicity⁶⁰. In this study, the concentrations of LDH released from all healthy HOF and HOK cells relative to the lysed cells (which is assigned to 100%) were greater than their attachment on S-PLCL and F-PLCL with various TC concentration membranes at 24 hours (Figure 7) would suggest. It appeared that the LDH activity of HOF cells was greater for S-PLCL for concentrations of TC loading up to 750 µg/ml. For higher TC-loaded concentrations, the LDH activity of F-PLCL was greater than that of S-PLCL, while LDH activity of HOK in TC-loaded S-PLCL was generally lower than TC-loaded F-PLCL. All attached cells demonstrated no significant differences when compared with healthy cells ($P > 0.05$). These results suggest that membranes of S-PLCL and F-PLCL with various TC-loadings were not cytotoxic to HOF and HOK cells. This outcome was consistent with the FDA status of the PLCL polymer combined with suitable

concentrations of TC drug release, which effectively promoted cell adhesion and proliferation.

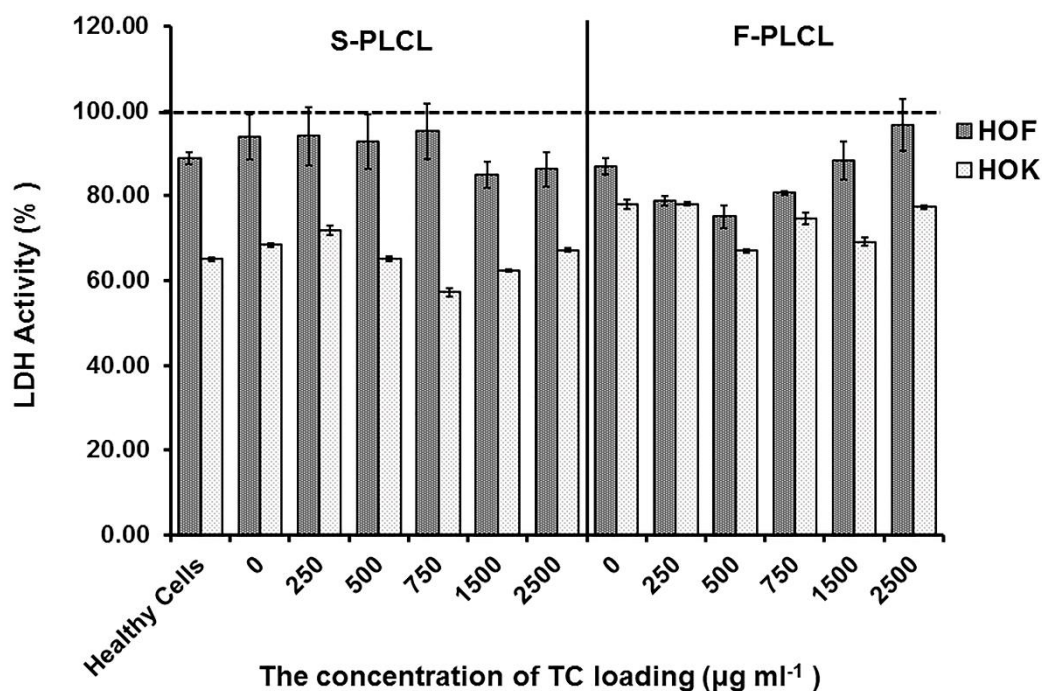


Figure 7. Membrane integrity (LDH assay) of (■) HOF and (□) HOK cells cultivated on S-PLCL and F-PLCL membranes with various TC-loading values for 24 hours with lysed cells assigned at 100%

3.6. Colony Forming Unit in Plaque Inhibition

In this study, the minimum inhibitory concentration (MIC) and the minimum bactericidal concentration (MBC) of TC were determined using the broth dilution method⁶¹. The MIC and MBC values recorded for TC loadings that inhibited the visible growth of plaque from the patients tested were found to be 30 and 375 µg/mL, respectively. In this study, the plaque samples from three patients were studied without bacterial isolation and identification. The bacteria associated with periodontal diseases are, however, predominantly gram-negative anaerobic bacteria and may include *A. actinomycetemcomitans*, *P. gingivalis*, *P. intermedia*, *B. forsythus*, *C. rectus*, *E. nodatum*, *P. micros*, *S. intermedius* and *Treponema sp*²².

The S-PLCL and F-PLCL membranes loaded with different concentrations of TC were investigated for antibacterial activity against the three different oral plaque samples.

After 24 hours of incubation under anaerobic conditions, the results indicated that TC in both membranes had an effect on all plaque samples, especially at concentrations of 1,500 and 2,500 $\mu\text{g/ml}$. No colony forming units were observed in any of the plaque samples at higher concentrations, as shown in Table 2, while the normal plaque suspension values observed in the control groups were 9.95, 9.76, and 10.18 CFU/ml in plaques no 1, 2 and 3, respectively. Previous research studies report that TC has a broad antibiotic spectrum that includes gram-negative and gram-positive microorganisms¹⁸⁻²⁰. Hence, the amount of TC released from all membranes can inhibit both negative and positive grams of unidentified microorganisms in the plaque samples. TC loaded in the F-PLCL membrane was somewhat more effective at inhibiting infection in the three plaque samples compared to the S-PLCL membrane. A minimum TC-loading of 750 $\mu\text{g/ml}$ in F-PLCL was required to inhibit plaque colony forming. The S-PLCL membranes contained 1,500 $\mu\text{g/ml}$, a greater amount than this. The cytotoxic results indicate that the S-PLCL loaded TC was less toxic compared to F-PLCL, as has been described in the previous section. Thus, when compared with the F-PLCL membrane, the S-PLCL material controlled and released the TC drug to a suitable degree and was determined to be non-toxic. It displayed no bacterial inhibition, while the best initial TC loading value for S-PLCL was 1,500 $\mu\text{g/ml}$.

Table 2 Plaque inhibition values as colony forming units on S-PLCL and F-PLCL membranes with various TC drugs

Log colonies (CFU/ml)						
[TC]	Plaque 1		Plaque 2		Plaque 3	
	S-PLCL	F-PLCL	S-PLCL	F-PLCL	S-PLCL	F-PLCL
0	9.75±0.2	9.89±0.3	9.46±0.2	9.98±0.6	9.91±0.3	8.52±0.3
250	9.90±0.1	9.20±0.2	9.26±0.5	0.00±0.0	9.90±0.8	7.49±0.2
500	7.10±0.6	3.30±0.4	8.24±0.4	0.00±0.0	7.93±0.2	0.00±0.0
750	0.00±0.0	0.00±0.0	0.00±0.0	0.00±0.0	7.09±0.	0.00±0.0
1500	0.00±0.0	0.00±0.0	0.00±0.0	0.00±0.0	0.00±0.0	0.00±0.0
2500	0.00±0.0	0.00±0.0	0.00±0.0	0.00±0.0	0.00±0.0	0.00±0.0
Control	9.95±0.1		9.76±0.2		10.18±0.3	

(CFU/ml) **Colony forming unit:** CFU is a measurement of viable bacterial or fungal cells in a given sample. For the purposes of convenience, the results are presented as CFU/ml (colony-forming units per millilitre).

4. CONCLUSIONS

The results of this study of a one-step modified periodontal membrane have been promising in terms of its safety and potential to provide benefits to patients. The variation of TC loading in the resorbable PLCL membranes has resulted in significant effects on the hydrophilicity in term of water contact angle and the water vapor transmission rate but did not effect on the fiber diameters. The loading of TC in S-PLCL membranes significantly lowered cell cytotoxicity and more efficiently promoted cell growth compared to F-PLCL membranes. The fabricated prototypes effectively facilitated the controlled release of TC over a suitable amount of time, while both treatments were determined to be anti-biotic. The fabricated S-PLCL loaded with 1,500 ppm of TC released 30 ppm of the drug. Additionally, it effectively promoted human oral fibroblast (HOF) and human oral keratinocyte (HOK) cell proliferation to an even greater degree. These results correspond to the % viability of the cells and their % membrane integrity. The TC drug-loaded S-PLCL membranes, especially at 1,500 $\mu\text{g/ml}$, displayed effective antibacterial activity against all of the oral plaque samples. Therefore, the developed TC-loaded S-PLCL membranes displayed effective potential in applications for periodontal treatment.

Supporting Information:

Chemical structures of (a) poly(L-lactide-*co*- ϵ -caprolactone), PLCL and (b) tetracycline, TC (Figure S1); chromatogram of residual L-Lactide and ϵ -caprolactone monomer in the medical-grade poly(L-lactide-*co*- ϵ -caprolactone) (PLCL) copolymer, as determined by gas chromatography with a flame ionization detector (GC-FID) using methylene chloride as solvent and 2,6-dimethyl- α -pyrone as an internal standard (Figure S2); the results of residual L-Lactide (LL) monomer in medical-grade poly(L-lactide-*co*- ϵ -caprolactone) (PLCL) (n=3) (Table S1); The results of residual ϵ -caprolactone (CL) monomer in medical-grade poly(L-lactide-*co*- ϵ -caprolactone) (PLCL) (n=3) (Table S2); Photographs of (a) solvent cast film (F-PLCL) (b) electrospun membrane (S-PLCL) and SEM images of (c) solvent cast film (F-PLCL) and (d) electrospun membrane (S-PLCL) (Magnification $\times 4000$) (Magnification $\times 4000$, thick black bar equal 5 μm) (Figure S3)

ACKNOWLEDGEMENTS

This research was financially supported by the Program Management Unit for Human Resources & Institutional Development, Research and Innovation, Office of National Higher Education Science Research and Innovation Policy Council (NXPO) [Grant Number B16F640001], the Center for Innovation in Chemistry (PERCH-CIC) and Center of Excellence in Materials Science and Technology, Chiang Mai University. This project also received funding from the European Union's Horizon 2020 research and innovation programme under Marie Skłodowska-Curie grant agreement No. 871650 (MEDIPOL).

REFERENCES

- [1] Kothari, S.; Gnanaranjan, G.; Kothiyal, P. Periodontal chip: an adjunct to conventional surgical treatment. *International Journal of Drug Research and Technology*. 2012, 2(6), 411-421.
- [2] Bottino, M.C.; Thomas, V.; Schmidt, G.; Vohra, Y.K.; Chu, T.M.G.; Kowolik, M.J.; Janowski, G.M. Recent advances in the development of GTR/GBR membranes for periodontal regeneration-A materials perspective. *Dental Materials*. 2012, 28, 703-721.
- [3] Bostanci, N.; Belibasakis, G.N. Doxycycline inhibits TREM-1 induction by *Porphyromonas gingivalis*. *Immunology and Medical Microbiology*. 2012, 66, 37-44.
- [4] Varanat, M.; Haase, E.M.; Kay, J.G.; Scannapieco, F.A. Activation of the TREM-1 pathway in human monocytes by periodontal pathogens and oral commensal bacteria. *Molecular Oral Microbiology*. 2017, 32, 275-287.
- [5] Slots, J.; Chen, C. The oral microflora and human periodontal disease. In: Tannock GW, ed. *Medical Importance of the Normal Microflora*. London. Kluwer Academic Publishers. 1999, 101-127.
- [6] Mundargi, R.C.; Srirangarajan, S.; Agnihotri, S.A.; Patil, S.A.; Ravindra, S.; Setty, S.B.; Aminabhavi, T.M. Development and evaluation of novel biodegradable microspheres based on poly(D, L-lactide-co-glycolide) and poly(ϵ -caprolactone) for controlled delivery of doxycycline in the treatment of human periodontal pocket: In vitro and in vivo studies. *Journal of Controlled Release*. 2007, 119, 59-68.
- [7] Ramesh, A.; Prakash, A.P.; Thomas, B. Local Drug Delivery in periodontal diseases. *Nitte University Journal of Health Science*. 2016, 6(1), 74-79.
- [8] Ulery, B.D.; Nair, L.S.; Laurencin, C.T. Biomedical applications of biodegradable polymers. *Journal of Polymer Science Part B: Polymer Physics*. 2011, 49(12), 832-864.

- [9] Pihlstrom, B.L.; Michalowicz, B.S; Johnson, N.W. Periodontal diseases. *Lancet* 2005, 366(9499), 1809-1820.
- [10] Nakashima, M A.; H. Reddi. The application of bone morphogenetic proteins to dental tissue engineering. *Nature Biotechnology*. 2003, 21(9), 1025-1032.
- [11] Nanci, A.; Bosshardt, D.D. Structure of periodontal tissues in health and disease. *Periodontology* 2000. 2006, 40, 11-28.
- [12] Slots, J.; Jorgensen, M.G. Efficient antimicrobial treatment in periodontal maintenance care. *Journal of the American Dental Association*. 2000, 131, 1293-1304.
- [13] Akcakanat, E.G.; Gurgan, C.A. Systemic moxifloxacin vs amoxicillin/metronidazole adjunct to non-surgical treatment in generalized aggressive periodontitis. *Medicina Oral Patologia Oral y Cirugia Bucal*. 2015, 20(4), e441-e449.
- [14] Slots, J. Systemic antibiotics in periodontics. *Journal of Periodontology*. 1991, 75(11), 1553-1565.
- [15] Baker, P.J.; Evans, R.T.; Slots, J.; Genco, R.J. Susceptibility of human oral anaerobic bacteria to antibiotics suitable for topical use. *Journal of Clinical Periodontology*. 1985, 12(3), 201-208.
- [16] Silverstein, L.; Bissada, N.; Manouchehr, P.M.; Greenwe, H. Clinical and Microbiologic Effects of Local Tetracycline Irrigation on Periodontitis. *Clinical and Microbiologic*. 1988, 59(5), 301-305.
- [17] Jorgensen, J.H.; Ferraro, M.J. Antimicrobial susceptibility testing: a review of general principles and contemporary practices. *Clinical Infectious Diseases*. 2009, 49(11), 1749-1755.
- [18] Shao, W.; Wang, S.; Liu, X.; Liu, H.; Wu, J.; Zhang, R.; Huang, M. Tetracycline hydrochloride loaded regenerated cellulose composite membranes with controlled release and efficient antibacterial performance. *Royal Society of Chemistry Advances*. 2016, 6(4), 3068-3073.
- [19] Shahi, R.G.; Albuquerque, M.T.P.; Münchow, E.A. Novel bioactive tetracycline-containing electrospun polymer fibers as a potential antibacterial dental implant coating. *Odontology*. 2017, 105, 354–363.
- [20] Tariq, S.; Rizvi S.F. A.; Anwar, U. Tetracycline: Classification, Structure Activity Relationship and Mechanism of Action as a Theranostic Agent for Infectious Lesions-A Mini Review. *Biomedical Journal of Scientific & Technical Research*. 2018, 7(2): 5787-5796.

- [21] Reneker, D.H.; Yarin, A.L. Bending instability of electrically charged liquid jets of polymer solutions in electrospinning. *Journal of Applied Physics*. 2000, 87(9), 4531-4547.
- [22] Kenawy, E.R.; Bowlin, G.L., Mansfield, K.; Layman, J.; Simpson, D.G.; Sanders, E.H.; Wnek, G. E. Release of tetracycline hydrochloride from electrospun poly(ethylene-co-vinylacetate), poly(lactic acid), and a blend. *Journal of Controlled Release*. 2002. 81(1-2), 57-64.
- [23] Reneker, D.H.; Chun, I. Nanometer diameter fibers of polymers, produced by electrospinning. *Nanotechnology*. 1996, 7, 216-223.
- [24] Buchko, C.J.; Chen, L.C.; Shen, Y.; Martin, D.C. Processing and microstructural characterization of porous biocompatible protein polymer thin films. *Polymer*. 1999, 40, 7397.
- [25] Huang, L.; McMillan, R.A.; Apkarian, R.P.; Pourdeyhimi, B.; Conticello, V.P.; Chaikoff, E.L. Generation of synthetic conelastin-mimetic small diameter fibers and fiber networks. *Macromolecules*. 2000, 33, 2989-2997.
- [26] Wang, L.; Topham, P.D.; Mykhaylyk, O.O.; Yu, H.; Ryan, A.J.; P.A, J. Fairclough, W Bras. Self-Assembly-Driven Electrospinning: The Transition from Fibers to Intact Beaded Morphologies. *Macromolecular Rapid Communications*, 2015, 36(15), 1437-1443.
- [27] Chen, L.; Wang, S.; Yu, Q.; Topham, P.D.; Chen, C.Z.; Wang, L. A Comprehensive Review of Electrospinning Block Copolymers. *Soft Matter*. 2019, 15, 2490-2510.
- [28] Li, W.; Yu, Q.; Yao, H.; Zhu, Y.; Topham, P.D.; Yue, K.; Ren, L.; Wang, L. Superhydrophobic hierarchical fiber/bead composite membranes for efficient burns treatment. *Acta Biomaterialia*. 2019, 92, 60-70.
- [29] Jia, Y.; Yang, C.; Chen, X.; Xue, W.; H-Crawford, H.J.; Yu, Q.; Topham, P.D.; Wang, L. A review on electrospun magnetic nanomaterials: methods, properties and applications. *Journal of Materials Chemistry C*. 2021, 9, 9042-9082.
- [30] Aliko, K.; Aldakhlalla, M.B.; Leslie, L.J.; Worthington, T.; Topham, P.D.; Theodosiou, E. Poly(butylene succinate) fibrous dressings containing natural antimicrobial agents. *Journal of Industrial Textiles*. 2021, 0(0), 1-20.
- [31] Zahedi, P.; Karami, Z.; Rezaeian, I.; Jafari, S.H.; Mahdavian, P.; Abdolghaffari, A. H.; Abdollahi, M. Preparation and performance evaluation of tetracycline hydrochloride loaded wound dressing mats based on electrospun nanofibrous poly(lactic acid)/poly(ϵ -caprolactone) blends. *Journal of Applied Polymer Science*. 2011, 124(5), 4174-4183.





- [32] Daranarong, D.; Techaikool, P., Intatue, W.; Daengngern, R.; Thomson, K.A., Molloy, R.; Punyodom, W. Effect of surface modification of poly(l-lactide-co- ϵ -caprolactone) membranes by low-pressure plasma on support cell biocompatibility. *Surface and Coatings Technology*. 2016. 306. 328-335.
- [33] Thapsukhon, B.; Daranarong, D.; Meepowpan, P.; Suree, N.; Molloy, R.; Inthanon, K.; Punyodom, W. Effect of topology of poly(L-lactide-co- ϵ -caprolactone) scaffolds on the response of cultured human umbilical cord Wharton's jelly-derived mesenchymal stem cells and neuroblastoma cell lines. *Journal of Biomaterials Science, Polymer Edition*. 2014, 25(10), 1028-1044.
- [34] Thapsukhon, B.; Thadavirul, N.; Supaphol, P.; Meepowpan P.; Molloy, R.; Punyodom, W. Effects of copolymer microstructure on the properties of electrospun poly(l-lactide-co- ϵ -caprolactone) absorbable nerve guide tubes. *Journal of Applied Polymer Science*. 2013; 4357-4366.
- [35] Daranarong, D.; Chan, R.T.H.; Wanandy, N.S.; Molloy, R.; Punyodom, W.; Foster, L.J.R. Electrospun Polyhydroxybutyrate and Poly(L-lactide-co- ϵ -caprolactone) Composites as Nanofibrous Scaffolds. *BioMed Research International*. 2014; 1-12.
- [36] American Society for Testing and Materials (ASTM). 2017. Standard Specification for Semi-Crystalline Poly(lactide) polymer and Copolymer Resins for Surgical Implants: ASTM F1925-17.
- [37] Shiku, Y.; Hamaguchi, P.Y.; Benjakul, S.; Visessanguan, W.; Tanaka, M. Effect of surimi quality on properties of edible films based on Alaska pollack. *Food Chemistry*. 2004; 86: 493-499.
- [38] P. Karuppuswamy, J.R. Venugopal, B. Navaneethan, A.L. Laiva, S. Ramakrishna. Polycaprolactone nanofibers for the controlled release of tetracycline hydrochloride. *Materials Letters*. 2015; 141: 180-186.
- [39] Barnett, S.C. Olfactory ensheathing cells: unique glial cell types. *Journal of Neurotraum*. 2004; 21: 375-382.
- [40] United STATES Patent US5501959. Antibiotic and cytotoxic drug susceptibility assays using resazurin and poisoning agents. *Biotechnology Advances*. 1995; 15(1): 193.
- [41] Braydich-Stolle, L.; Hussain, S.; Schlager, J. J.; Hofmann, M.C. In Vitro Cytotoxicity of Nanoparticles in Mammalian Germline Stem Cells. *Toxicological Sciences*. 2005; pp(88): 412-419.

- [42] Kooltheat, N.; Kamuthachad, L.; Anthapanya, M.; Samakchan, N.; Sranujit, R.P.; Potup, P.; Usuwanthim, K. Kaffir lime leaves extract inhibits biofilm formation by *Streptococcus mutans*. *Nutrition*. 2016; 32(4): 486-490.
- [43] Clinical and Laboratory Standards Institute. *Methods for dilution antimicrobial susceptibility tests for bacteria that grow aerobically*; approved standard ninth edition. Pennsylvania: Clinical and Laboratory Standards Institute; 2012.
- [44] Hamid, R.; Rotshetyn, Y.; Rabadi, L.; Parikh, R.; Bullock P.; Comparison of alamar blue and MTT assays for high through-put screening. *Toxicology in Vitro*. 2004; 18(5): 703-710.
- [45] Palmieri, S.; Tittarelli, F.; Sabbatini, S.; Cespi, M.; Bonacucina, G.; Eusebi, A.L.; Fatone, F.; Stipa, P. Effects of different pre-treatments on the properties of polyhydroxyalkanoates extracted from sidestreams of a municipal wastewater treatment plant. *Science of The Total Environment*. 2021, Volume 801,149633.
- [46] Molina, M.I.E.; Malollari, K.G.; Komvopoulos, K. Design Challenges in Polymeric Scaffolds for Tissue Engineering. *Frontiers in Bioengineering and Biotechnology*. 9, 2021, 617141.
- [47] Wu, J; Li, X.; Wu, Y.; Liao, G.; Johnston, P.; Topham, P.D.; Wang, L. Rinse-resistant superhydrophobic block copolymer fabrics by electrospinning, electrospraying and thermally-induced self-assembly. *Applied Surface Science*. 2017; S0169-4332(17): 31731-2.
- [48] Gould, R.F. *Contact Angle, Wettability, and Adhesion*, Advances in Chemistry Series, American Chemical Society, 1964.
- [49] Tipachan, C.; Gupta, R.K.; Kajorncheappunngam, S. Water vapor barrier property of PLA nanocomposites using rice husk ash and layered double hydroxides as fillers. *Engineering and Applied Science Research*. 2019; 46(4): 285-291.
- [50] Duan, Z.; Thomas, N.L.; Huang, W. Water vapour permeability of poly(lactic acid). *Journal of Membrane Science*. 2013; 445: 112-118.
- [51] Müller, K.; Bugnicourt, E.; Latorre, M.; Jorda, M.; Echevoyen Sanz, Y.; Lagaron, J.M.; Miesbauer, O.; Bianchin, A.; Hankin, S.; Bölz, U.; Pérez, G.; Jesdinszki, M.; Lindner, M.; Scheuerer, Z.; Castelló, S.; Schmid, M. Review on the Processing and Properties of Polymer Nanocomposites and Nanocoatings and Their Applications in the Packaging, Automotive and Solar Energy Fields. *Nanomaterials*. 2017, 7, 74.

- [52] Kiaee, G.; Etaat, M.; Kiaee, B., Kiaei, S.; Javar, H.A. Multilayered controlled released topical patch containing tetracycline for wound dressing. *Journal of In Silico & In Vitro Pharmacology*. 2016; 2(2): 1-7.
- [53] Soares, J.S.; Zunino, P. A mixture model for water uptake, degradation, erosion and drug release from polydisperse polymeric networks. *Biomaterials*. 2010; 31: 3032-3042.
- [54] Ciarfaglia, N.; Laezza, A.; Lods, L.; Lonjon, A.; Dandurand, J.; Pepe, A.; Bochicchio, B. Thermal and dynamic mechanical behavior of poly(lactic acid) (PLA)-based electrospun scaffolds for tissue engineering. *Journal of Applied Polymer Science*. 2021, 138 (44), art. no. 51313.
- [55] Wylie, C.M.; Davenport, A.J.; Cooper, P.R.; Shelton, R.M. Oral keratinocyte responses to nickel-based dental casting alloys *in vitro*. *Journal of Biomaterials Applications*. 2009; 25(3): 251-267.
- [56] Kowalczyk T. Functional Micro- and Nanofibers Obtained by Nonwoven Post-Modification. *Polymers (Basel)*. 2020, 10;12(5), 1087.
- [57] Park, B.S.; Heo, S.J., Kim, C.S., Oh, J.E.; Kim, J.M.; Lee, G.; Park, W.H.; Chung, C. P.; Min, B.M. Effects of adhesion molecules on the behavior of osteoblast-like cells and normal human fibroblasts on different titanium surfaces. *Journal of Biomedical Materials Research*. 2005; 74A: 640-651.
- [58] Oh, J. E.; Park, K.H.; Noh, H.K.; Kim, J. M.; Chung, C. P.; Min; B.M. Decreased expression of 3 and 1 integrin subunits is responsible for differentiation-associated changes in cells behavior in terminally differentiated human oral keratinocytes. *Cell Communication and Adhesion*. 2002; 9(4): 173-187.
- [59] Mu, X.; Agostinacchio, F.; Xiang, N.; Pei, Y.; Khan, Y.; Guo, C.; Cebe, P.; Motta, A.; Kaplan, D.L. Recent Advances in 3D Printing with Protein-Based Inks. *Prog Polym Sci*. 2021, 115, 101375.
- [60] Zuo, Y.; Yang, F.; Wolke, J.G.C.; Li, Y.; Jansen, J.A. Incorporation of biodegradable electrospun fibers into calcium phosphate cement for bone regeneration. *Acta Biomaterialia*. 2010; 6(4): 1238-1247.
- [61] Balouiri, M.; Sadiki, M.; Ibnsouda; S.K. Methods for in vitro evaluating antimicrobial activity: A review. *Journal of Pharmaceutical Analysis*. 2016; 6(2): 71-79.

“For Table of Contents Only”

Table of Contents

Table 1	Physical and chemical property measurements, compared with the ASTM F1925-17 specification, for the medical-grade PLCL copolymer.
Figure 1	(a) SEM images of electrospun nanofibrous meshes of S-PLCL and S-PLCL with various TC drug loadings (Magnification $\times 4000$, thick black bar equal 5 μm) and (b) changes in the average fiber diameter of S-PLCL membranes loaded with TC drug ($\mu\text{g/ml}$).
Figure 2	Effect of TC drug loading on the water contact angle of PLCL electrospun fabric (S-PLCL) and film (F-PLCL) membranes.
Figure 3	Water vapor permeability (WVP) of (a) S-PLCL and (b) F-PLCL membranes at TC loadings of 0, 250, 500, 750, 1,500 and 2,500 $\mu\text{g/ml}$
Figure 4	Time and TC drug release of (a) S-PLCL and (b) F-PLCL membranes at various degrees of TC loading
Figure 5	Weight retention values for the (a) S-PLCL and (b) F-PLCL membranes and pH decreases for (c) S-PLCL and (d) F-PLCL membranes in accordance with various TC drug loading concentration in $\mu\text{g/ml}$ during <i>in vitro</i> hydrolytic degradation
Figure 6	Indirect cell metabolic activity of () HOF and () HOK cells cultivated on S-PLCL and F-PLCL membranes at various TC-loading values for 24 hours measured by alamarBlue assay, with cells in asynchronous growth assigned at 100%.
Figure 7	Membrane integrity (LDH assay) of () HOF and () HOK cells cultivated on S-PLCL and F-PLCL membranes with various TC-loading values for 24 hours with lysed cells assigned at 100%
Table 2	Plaque inhibition values as colony forming units on S-PLCL and F-PLCL membranes with various TC drugs